

**Acute diabetes moderates trafficking of cardiac lipoprotein lipase through p38
MAPK dependent actin cytoskeleton organization**

Min Suk Kim, Girish Kewalramani, Prasanth Puthanveetil, Vivian Lee, Ujendra Kumar,
Ding An, Ashraf Abrahani, and Brian Rodrigues

Division of Pharmacology and Toxicology, Faculty of Pharmaceutical Sciences,
The University of British Columbia, 2146 East Mall, Vancouver, BC, Canada V6T 1Z3

Running title: Stress kinases and LPL

Corresponding author:

Dr. B. Rodrigues

Division of Pharmacology and Toxicology

Faculty of Pharmaceutical Sciences

The University of British Columbia

2146 East Mall, Vancouver, B.C., Canada V6T 1Z3

E-mail: rodrigue@interchange.ubc.ca

Received for publication 20 June 2007 and accepted in revised form 11 October 2007.

ABSTRACT

Objective. Heart disease is a leading cause of death in diabetes, and could occur due to excessive utilization of fatty acid (FA) for energy generation. Our objective was to determine the mechanisms by which AMPK augments cardiac lipoprotein lipase (LPL), the enzyme that provides the heart with majority of its FA.

Research Design and Methods. We used diazoxide (DZ) in rats to induce hyperglycemia, or AICAR and thrombin to directly stimulate AMPK and p38 MAPK respectively in cardiomyocytes.

Results. There was a substantial increase in LPL at the coronary lumen following 4 h of DZ. In these diabetic animals, phosphorylation of AMPK, p38 MAPK, and Hsp25 produced actin cytoskeleton rearrangement to facilitate LPL translocation to the myocyte surface, and eventually the vascular lumen. AICAR activated AMPK, p38 MAPK, and Hsp25 in a pattern similar to that seen with diabetes. AICAR also appreciably enhanced LPL, an effect reduced by pre-incubation with the p38 MAPK inhibitor SB202190, or cytochalasin D that inhibits actin polymerization. Thrombin activated p38 MAPK in the absence of AMPK phosphorylation. Comparable to diabetes, activation of p38 MAPK, and subsequently, Hsp25 phosphorylation and F-actin polymerization corresponded with an enhanced LPL activity. SB202190 and silencing of p38 MAPK also prevented these effects induced by thrombin and AICAR respectively.

Conclusions. We propose that AMPK recruitment of LPL to the cardiomyocyte surface (which embraces p38 MAPK activation and actin cytoskeleton polymerization) represents an immediate compensatory response by the heart to guarantee FA supply when glucose utilization is compromised.

KEY WORDS

Heart, Fatty Acids, AMPK, Hsp25, AICAR

Heart disease is a leading cause of death in diabetic patients (1), with coronary vessel disease and atherosclerosis being primary reasons for the increased incidence of cardiovascular dysfunction (2). However, a predisposition to heart failure in patients with both Type 1 and Type 2 diabetes might also reflect the effects of underlying abnormalities in diastolic function that can be detected in asymptomatic patients with diabetes alone (3-5). These observations suggest a specific impairment of heart muscle, termed diabetic cardiomyopathy. As rodent models of chronic diabetes also display abnormalities in diastolic left ventricular function, with or without systolic left ventricular dysfunction (6), it can be proposed that the diabetic state can directly induce abnormalities in cardiac tissue independent of vascular defects. Several etiological factors have been put forward to explain the development of diabetic cardiomyopathy including an increased stiffness of the left ventricular wall associated with accumulation of connective tissue and insoluble collagen (7), and abnormalities of various proteins that regulate ion flux, specifically intracellular calcium (8). More recently, the view that diabetic cardiomyopathy could also occur as a consequence of metabolic alterations has been put forward (9).

During insulin resistance or diabetes, glucose utilization is compromised. This alteration, together with increased fatty acid (FA) supply, switches cardiac energy generation to utilization of FA. High FA uptake and metabolism not only augments accumulation of FA intermediates and triglyceride (TG), but also increases oxygen demand and generation of reactive oxygen species, leading to cardiac damage. Interestingly, increasing FA uptake through overexpression of cardiac human lipoprotein lipase (LPL) (10) or fatty acid transport protein (11), or augmenting FA oxidation

through overexpression of cardiac PPAR- α (12) or long-chain acyl CoA synthase (13), results in a cardiac phenotype resembling diabetic cardiomyopathy. Conversely, normalizing cardiac metabolism in diabetic animals reverses the development of cardiomyopathy (14). Taken together, these studies strongly support the role of altered metabolism in the development of diabetic cardiomyopathy.

LPL hydrolyzes triglyceride (TG) rich lipoproteins, thus regulating the supply of FA to meet the metabolic demands of different tissues. It is synthesized in myocytes and subsequently transported onto heparan sulfate proteoglycan (HSPG) binding sites on the myocyte cell surface (15). Through mechanisms that are not completely understood, LPL is then transported onto HSPG binding sites on the luminal surface of the capillary endothelium (16). At this location, the enzyme plays a crucial role in hydrolysis of TG rich lipoproteins to FA, which are transported to the heart and used either for energy production or for re-synthesis of TG. Recently, LPL-mediated hydrolysis of circulating TG was suggested to be the principal source of FA for cardiac utilization (17,18). In addition to its role as a lipolytic enzyme, LPL also mediates a non-catalytic bridging function that allows it to bind simultaneously to both lipoproteins and specific cell surface proteins, facilitating cellular uptake of lipoproteins (19).

AMP activated protein kinase (AMPK) plays a key role in the regulation of cardiac metabolism. Once activated, AMPK switches off energy consuming processes like protein synthesis, whereas ATP generating mechanisms, such as FA oxidation and glycolysis, are turned on (20). Additionally, results from our laboratory have demonstrated a strong correlation between activation of AMPK and increases in LPL activity (21). The objective of the present study was to determine the mechanisms by which AMPK

augments cardiac LPL. Our data demonstrates that stress kinases like AMPK and p38 mitogen-activated protein kinase (MAPK), through their control of heat shock protein (Hsp) and the actin cytoskeleton, act in unison to facilitate LPL translocation to the myocyte cell surface, and eventually to the coronary lumen. The ensuing alteration in cardiac FA metabolism could be translated into increased cardiovascular risk following diabetes.

RESEARCH DESIGN AND METHODS

Experimental animals. The investigation conforms to the guide for the care and use of laboratory animals published by the US National Institutes of Health and the University of British Columbia. Adult male Wistar rats (260-300 g) were obtained from the UBC Animal Care Unit and supplied with a standard laboratory diet (PMI Feeds, Richmond, VA), and water ad libitum. Diazoxide (DZ), a selective K^+_{ATP} channel opener, decreases insulin secretion and causes hyperglycemia (22,23). Although doses of 25 and 50 mg/kg increased plasma glucose, the extent and duration of hyperglycemia were not as substantial as that seen with 100 mg/kg, which caused a rapid decline in serum insulin within 1 h (23). DZ (100 mg/kg) was administered i.p., and animals were euthanized at various times. Subsequently, hearts were removed for measurement of coronary luminal LPL activity and Western blotting.

Plasma measurements. Control rats were injected with DZ at 10 AM (fed state). Following DZ, blood samples from the tail vein were collected over a period of 4 h, and blood glucose determined using a glucometer (AccuSoft) and glucose test strips (Accu-Chek Advantage, Roche). At varying intervals, blood was also acquired in heparinized glass capillary tubes. Blood samples were immediately centrifuged and plasma was collected and assayed. A

diagnostic kit was used to measure non-esterified fatty acid (NEFA, Wako).

Isolated heart perfusion. Rats were anesthetized with 65 mg/kg sodium pentobarbital i.p., the thoracic cavity opened, and the heart carefully excised. Following cannulation of the aorta, hearts were secured by tying below the innominate artery and perfused retrogradely by the nonrecirculating Langendorff technique with Krebs-Henseleit buffer containing 10 mM glucose (pH 7.4). Perfusion fluid was continuously gassed with 95% O_2 /5% CO_2 . The rate of coronary flow (7-8 ml/min) was controlled by a peristaltic pump (24).

LPL activity and gene and protein expression. To measure coronary endothelium-bound LPL, the perfusion solution was changed to buffer containing fatty acid free BSA (1%) and heparin (5 U/ml). This concentration of heparin can maximally release cardiac LPL from its HSPG binding sites. The coronary effluent (perfusate that drips down to the apex of the heart) was collected in timed fractions (10 sec) over 5 min, and assayed for LPL activity by measuring the hydrolysis of a [3H] triolein substrate emulsion (25). Retrograde perfusion of whole hearts with heparin results in a discharge of LPL that is rapid (within 0.5 to 1 min; suggested to represent LPL located at or near the endothelial cell surface) followed by a prolonged slow release (that is considered to originate from the myocyte cell surface) (24). As we were primarily concerned with examining regulation of LPL at coronary lumen, only peak LPL activities are illustrated. LPL activity is expressed as nanomoles oleate released per hour per milliliter. LPL gene expression was measured using RT-PCR (26), and protein expression was determined using the 5D2 monoclonal mouse anti-bovine LPL (generously provided by Dr. J. Brunzell, University of Washington, Seattle, WA) (^{27; 28}).

Western blotting. Western blot was carried out as described previously (21). Briefly,

ventricles (50 mg) or plated myocytes (0.4×10^6) were homogenized in ice-cold lysis buffer. After centrifugation at 5,000 g for 20 min, the protein content of the supernatant was quantified using a Bradford protein assay. Samples were diluted, boiled with sample loading dye, and 50 μ g used in SDS-polyacrylamide gel electrophoresis. After blotting, membranes were blocked in 5% skim milk in Tris-buffered saline containing 0.1% Tween-20. Membranes were incubated either with rabbit AMPK- α , phospho-AMPK (Thr-172), p38 MAPK, phospho-p38 MAPK (Thr180/Tyr182), Hsp25, and phospho-Hsp25 (S86) antibodies, and subsequently with secondary goat anti-rabbit HRP-conjugated antibody. Reaction products were visualized using an ECL[®] detection kit, and quantified by densitometry.

Isolated cardiac myocytes. Ventricular calcium-tolerant myocytes were prepared by a previously described procedure (23,28). Briefly, myocytes were made calcium-tolerant by successive exposure to increasing concentrations of calcium. Our method of isolation yields a highly enriched population of calcium-tolerant myocardial cells that are rod-shaped in the presence of 1 mM Ca^{2+} with clear cross striations. Intolerant cells are intact but hypercontract into vesiculated spheres. Yield of myocytes (cell number, $\sim 4.8 \times 10^6$) was determined microscopically using an improved Neubauer haemocytometer. Myocyte viability (generally between 75-85%) was assessed as the percentage of elongated cells with clear cross striations that excluded 0.2% trypan blue. To examine the influence 5-aminoimidazole-4-carboxamide-1- β -D-ribofuranoside (AICAR, an AMPK activator) and the serine protease thrombin (to activate p38 MAPK) on LPL activity, cardiomyocytes were plated on laminin-coated 6-well culture plates (to a density of 200,000 cells/well). Cells were maintained using Media-199, and incubated at 37°C under an atmosphere of 95% O_2 /5% CO_2 for 16 hours. Subsequently,

and where indicated, AICAR (2 mM) or thrombin (0.05 U/ml) was added to the culture medium. Following the indicated times, myocyte basal LPL activity released into the medium was measured. To release surface-bound LPL activity, heparin (8 U/mL; 1 min) was added to the culture plates, aliquots of cell medium removed, separated by centrifugation, and assayed for LPL activity. In separate experiments, following incubation of plated myocytes (0.4×10^6 cells in a 60 x 15 mm tissue culture dish) with AICAR or thrombin, myocyte cell lysates were also used for Western blotting. In addition, myocytes were: a) pre-incubated with a p38 MAPK inhibitor (SB202190, 20 μ M) for 60 min prior to addition of either AICAR or thrombin (at the indicated times) and LPL activity and phospho-Hsp25 determined, or b) incubated with 0.5-1.5 mM albumin bound palmitic acid (1:2) for 15 mins prior to Western blotting for AMPK.

Nuclear localization of p38 MAPK. Following DZ, heart tissue was homogenized whereas after incubation of myocytes with thrombin, cells were scraped and washed twice with 0.5 ml PBS. Subsequently, samples were lysed in ice-cold buffer A (10 mM HEPES pH 7.9, 10 mM KCl, 0.1 mM EDTA, 0.1 mM EGTA 1 mM DTT, 0.5 mM PMSF and 0.5 % NP40) for 15 min. After centrifugation (13,000 rpm, 3 min, 4°C), the supernatant (cytosolic fraction) was separated, and the pellet vigorously vortexed with buffer B (20 mM HEPES pH 7.9, 0.42 M NaCl, 1 mM EDTA, 1 mM EGTA, 1 mM DTT, 1 mM PMSF) for 10 min. Following centrifugation (13,000 rpm, 10 min, 4°C), the supernatant (nuclear fraction) was quantified using a Bradford protein assay, and used for Western blotting to determine nuclear localization of p38 MAPK. Using an antibody against Histone H3 as a nuclear marker, we show good purity of nuclear fractions (data not shown).

Filamentous (F) and globular (G) actin. F-actin/G-actin ratio in the whole heart was

determined using an in vivo assay kit. Briefly, hearts from control and DZ animals were isolated and lysed. Lysates were homogenized and centrifuged at 2000 rpm for 5 min. Total actin content of the supernatant was centrifuged at 100,000 g for 1 hr at 37°C to isolate F-actin (pellet) and G-actin (supernatant). The pellets were re-suspended to same volume as the G-actin fraction using ice-cold Milli-Q water plus 10 μ M cytochalasin D, and left on ice for 1 hr to dissociate F-actin. The ratio of F-actin/G-actin was determined using western blotting and densitometry.

F-actin and G-actin was also determined in isolated cardiomyocytes using immunofluorescence. Briefly, myocytes were plated on laminin coated cover glass slides and rinsed with PBS. Following incubation with thrombin or SB202190 at the indicated times, myocytes were fixed for 10 min with 4% paraformaldehyde in PBS, permeabilized with 0.1% Triton X-100 in PBS for 3 min, treated with PBS containing 1% BSA for 20 minutes, and finally rinsed with PBS. Cells were double stained with DNAaseI AlexaFluor®594 and Rhodamine®488 Phalloidin to colocalize monomeric globular actin (red, G actin), and polymerized filamentous actin (green, F actin) (29). The unbound fluorescent probe was rinsed with PBS buffer and slides were visualized and photographed by using a Leica fluorescent microscope (Wetzlar, Postfach, Germany). The effects of AICAR in myocytes were also determined in the presence or absence of 1 μ M cytochalasin D (CTD; an actin polymerization inhibitor) (30).

Silencing of p38 MAPK by siRNA. siRNA transfection of p38 MAPK in cardiomyocytes was carried out using a kit from Santa Cruz. Briefly, in 6-well culture plates, 0.1×10^6 cells were plated and subsequently exposed to the siRNA (or scrambled, Scr) solution for 8h at 37°C in a CO₂ incubator. Following this, the media was changed to Media 199 and the cells incubated for another 18h.

Subsequently, AICAR (2 mM) was added to the culture medium for 2h, and LPL (released by heparin), p38 MAPK and Hsp25 (using Western blotting) were determined.

Materials. [³H]triolein was purchased from Amersham Canada. Heparin sodium injection (Hapalean; 1000 USP U/ml) was obtained from Organon Teknika. The F-actin/G-actin in vivo assay kit was obtained from Cytoskeleton Inc., Denver, CO. Total AMPK- α , Phospho-AMPK- α , p38 MAPK, phospho-p38 MAPK, GAPDH, and Histone H3 antibodies were obtained from Cell Signaling (Danvers, MA). Hsp25 and phospho-Hsp25 antibodies were obtained from GeneTex®, Inc. (San Antonio, TX). SB202190 was purchased from Sigma-Aldrich. ECL® detection kit was obtained from Amersham. A diagnostic kit was used to measure non-esterified fatty acid (NEFA, Wako). All other chemicals were obtained from Sigma Chemical.

Statistical analysis. Values are means \pm SE. Wherever appropriate, one-way ANOVA followed by the Bonferroni test was used to determine differences between group mean values. The level of statistical significance was set at $P < 0.05$.

RESULTS

Acute diabetes increases LPL at the vascular lumen. Following DZ, blood glucose levels increased, and were significantly higher at 1 and 4 h after administration (Fig. 1A). Another characteristic feature associated with hyperglycemia, such as polydipsia, was also observed in DZ treated animals. Retrograde perfusion of hearts with heparin resulted in release of LPL into the coronary perfusate. Compared to control rat hearts, there was a substantial increase in LPL activity (~400%, Fig. 1B) at the vascular lumen following 4 h of DZ. This change in LPL activity was independent of shifts in mRNA (data not shown), suggesting a posttranscriptional increase in myocyte LPL. In addition, as no change in whole heart LPL protein was

observed (data not shown), it is likely that the increase in LPL activity at the coronary lumen is simply due to transport of enzyme from myocytes to the endothelial cell. We have previously reported that control of LPL by DZ is dependent on its lowering of insulin rather than its direct effects on the heart or blood pressure (23).

Influence of fatty acids on cardiac AMPK phosphorylation. Previous studies from our lab have reported significantly higher AMPK phosphorylation in hearts from moderately diabetic STZ animals (31). In the present study, following DZ, an approximately 6-fold increase of cardiac AMPK phosphorylation was observed after 15 min (Fig. 2A). With time, despite persistence of hyperglycemia, AMPK phosphorylation in hearts from DZ treated animals declined, and reached basal levels within 4 h (Fig. 2A). As AMPK activation is prevented in severe STZ diabetes with its attendant enlargement of plasma and heart lipids (31), we measured changes in plasma FA to resolve whether a relationship exists between AMPK and FA in DZ treated animals. Interestingly, with time, the reduction in AMPK activation corresponded to a significant and rapid increase of FA that peaked at 60 min, and remained high until 4 h (Fig. 2B). When control myocytes were incubated with appropriate concentrations of palmitic acid, concentrations that varied from 0.5-0.8 mM activated cardiac AMPK (Fig. 2C). However, with high concentrations of palmitic acid (that resembled the peak circulating concentrations seen with DZ), activation of AMPK was absent (Fig. 2C), suggesting that *in vivo* and *in vitro*, FA has dual effects on AMPK activation.

Diazoxide stimulates cardiac actin polymerization. p38 MAPK, a downstream target of AMPK (32), is suggested to regulate actin polymerization through its phosphorylation of heat shock protein 25. In turn, the actin cytoskeleton has been implicated in managing myocyte LPL secretion (33). Estimation of cardiac

cytosolic p38 MAPK phosphorylation showed a similar pattern to that seen with activation of AMPK; rapid activation followed by a decline to control levels within 4 h (Fig. 3A). Once phosphorylated, p38 MAPK relocates to the nucleus (34). Separation of the nuclear fraction revealed that concurrent to the decline in cytosolic p38 MAPK phosphorylation, nuclear p38 MAPK phosphorylation increased (Fig. 3A, inset). Phosphorylation of Hsp25 also intensified (Fig. 3B). However, this increase was time dependent, reaching a maximum around 60 min and remaining elevated for the next 3 h. To determine whether Hsp25 phosphorylation elicits F-actin polymerization, we quantitated F-actin and G-actin cellular fractions using Western blot. In the resting cardiomyocyte, the proportion of polymerized F-actin is consistently higher than G-actin (90:10), and is predominantly localized along the cell periphery. Additionally, an increase in F-to-G actin ratio indicates actin polymerization. DZ increased the F/G actin ratio (Fig. 3C). Interestingly, the increase in F-actin polymerization closely mirrored the enlargement of LPL activity at 4 h after DZ (Fig. 1B).

Promotion of AMPK phosphorylation in isolated control myocytes activates p38 MAPK and Hsp25 and recruits LPL to the cardiomyocyte cell surface. To directly turn on AMPK, control myocytes were incubated for different times and with varying concentrations of AICAR. AICAR upto 1 mM was incapable of phosphorylating cardiac AMPK (data not shown). Interestingly, increasing the concentration to 2 mM activated AMPK phosphorylation in a pattern similar to that seen with acute diabetes; rapid activation followed by a decline to control levels with time (Fig. 4A). Comparable to acute diabetes induced with DZ, the activation of AMPK was temporally related to phosphorylation of p38 MAPK (Fig. 4B), and subsequently Hsp25 (Fig. 4C). We evaluated whether AICAR can augment LPL in

myocytes, and Table 1 illustrates both basal and heparin releasable LPL activity. Incubation of myocytes with AICAR had no effect on basal LPL activity. Interestingly, 2 mM AICAR appreciably enhanced heparin releasable activity in the medium. This increase occurred in the absence of any change in LPL mRNA or protein in cardiomyocyte lysates (data not shown).

We hypothesized that inhibition of Hsp25 phosphorylation should decrease cardiomyocyte LPL activity. In the absence of specific inhibitors of Hsp25, we used SB202190, an inhibitor of p38 MAPK. Incubation of control myocytes for 1 hour with SB202190 decreased Hsp25 phosphorylation that is produced by AICAR (Fig. 5A). More importantly, the robust increase in heparin-releasable LPL activity induced by AICAR was also reduced by pre-incubation of myocytes with SB202190 (Fig. 5B). To investigate the involvement of the actin cytoskeleton in AICAR-mediated augmentation of myocyte LPL, myocytes were pretreated with an actin polymerization inhibitor, CTD, before incubation with AICAR. CTD reduced the effect of AICAR to increase myocyte HR-LPL without any effect on basal activity (control-3417 \pm 181; AICAR-5305 \pm 223; AICAR+CTD-2163 \pm 178, nmol·h⁻¹·10⁻⁶ cells, $P < 0.05$).

Directly increasing p38 MAPK activity also enlarges the cardiomyocyte cell surface LPL pool. To activate p38 MAPK in the absence of AMPK phosphorylation, we used thrombin. As predicted, control myocytes in the presence of the serine protease thrombin did not display any change in AMPK phosphorylation (Fig. 6A, inset). Nevertheless, thrombin rapidly (within 5 min) phosphorylated cytosolic p38 MAPK, which was followed by a decline to control levels within 30 min. Comparable to diabetes, the decline in cytosolic p38 MAPK phosphorylation corresponded to an activation of nuclear p38 MAPK (Fig. 6B), Hsp25 phosphorylation (Fig. 6C), F-actin

polymerization (Fig. 8), and enhanced heparin releasable activity (Fig. 7B). Pre-incubation of control myocytes for 1 hour with SB202190 prevented all of these effects induced by thrombin (Fig. 7 and 8).

Silencing of p38 MAPK prevents cardiomyocyte LPL recruitment observed with AICAR. To confirm the relationship between p38 MAPK and LPL, we used short interfering RNA to silence p38 MAPK expression in isolated cardiomyocytes. We first validated successful p38 MAPK inhibition using Western blotting (Fig. 9, inset). Interestingly, in myocytes in which p38 MAPK was silenced, heparin releasable LPL activity was reduced (control+heparin-2308 \pm 150; p38 MAPK silenced control+heparin-1142 \pm 167, nmol·h⁻¹·10⁻⁶ cells, $P < 0.05$). Cardiomyocytes were next exposed to AICAR and Hsp25 and LPL activity determined. In myocytes in which p38 MAPK was silenced, AICAR had no influence on total p38 MAPK which remained low (Fig. 9A) and was unable to phosphorylate Hsp25 (Fig. 9B) or increase LPL activity (Fig. 9C).

DISCUSSION

The major source of FA for myocardial energy utilization is LPL mediated hydrolysis of TG-rich lipoproteins at the vascular endothelium (17). Despite this essential role of LPL at the coronary luminal surface, endothelial cells do not manufacture LPL. In the heart, the enzyme is synthesized in the underlying myocytes (35) before it is translocated to the luminal side of the coronary vessel wall with the help of heparan sulfate oligosaccharides acting as extracellular chaperones (¹⁶; ³⁶). Within the myocyte, we (30) and others (33) have reported actin cytoskeleton reorganization as an important means by which LPL is secreted onto plasma membrane HSPG binding sites. In this study, for the first time, we demonstrate that following diabetes, it is the phosphorylation of AMPK, p38 MAPK, and

Hsp25 that causes actin cytoskeleton rearrangement to facilitate LPL translocation to the myocyte cell surface, and eventually to the coronary lumen.

AMPK is the switch that regulates cellular energy metabolism (37). Changes in intracellular AMP/ATP levels promote Threonine (Thr¹⁷²) phosphorylation and activation of AMPK, an important regulator of both carbohydrate and lipid metabolism (38,39). Thus, in heart and skeletal muscle, phosphorylated AMPK stimulates glucose uptake by inducing GLUT4 recruitment to the plasma membrane (40,41) and subsequent glycolysis through activation of 6-phosphofructo-2-kinase (42). AMPK control of FA utilization includes its effect on FA delivery to cardiomyocytes through its regulation of CD36 (43), and its role in facilitating FA oxidation through its effect on acetyl-CoA carboxylase (ACC) (44). Recently, we have also demonstrated that following AMPK activation after overnight fasting (with its attendant hypoinsulinemia), heparin-releasable LPL activity is amplified providing an additional mechanism whereby cellular energy is regulated (21). In the present study, we report that acute diabetes increases cardiac LPL activity within four hours. This augmentation in LPL activity was preceded by a rapid and intense phosphorylation in AMPK, that was not sustainable, and declined to control levels at 4 hours. The early increase in AMPK may well be a product of either metabolic stress associated with a decrease in insulin, or a direct activation by circulating FFA. Interestingly, in studies using L6 skeletal muscle, FA's have been demonstrated to allosterically activate AMPK without changing energy charge (45). Despite the prevailing hyperglycemia following increasing durations of DZ, the decrease of AMPK activation to control levels is likely a consequence of the excessive amount of both circulating and LPL derived FA. This idea was strengthened by our experiment using

isolated myocytes incubated with high concentrations of palmitate. In addition, moderate diabetes significantly increases cardiac AMPK and ACC phosphorylation, whereas in severe diabetes, with the addition of augmented plasma and heart lipids, AMPK activation is prevented (31). Recently, high FA or TG, through their formation of ceramide, has been shown to activate protein phosphatase 2A leading to dephosphorylation of AMPK (46).

Given the observation that when LPL activity was the highest, AMPK phosphorylation had returned to normal, we considered the possibility that the early activation of AMPK may have turned on other downstream signals. One downstream target of AMPK is p38 MAPK, and there was coincident activation of both AMPK and p38 MAPK following injection of DZ. Other studies have demonstrated that AMPK activates p38 MAPK through its interaction with transforming growth factor- β -activated protein kinase 1-binding protein 1 (32). Cytosolic activation of p38 MAPK results in its transfer to the nucleus, and gene activation through a number of transcription factors (47). In the nucleus, p38 MAPK can also activate MAPKAP kinase 2, which is then exported to phosphorylate Hsp25. Our studies in the heart confirmed that cytosolic activation of p38 MAPK was followed by its nuclear translocation. More importantly, with increasing duration of hyperglycemia, phosphorylation of Hsp25 progressively increased. Hsp25 is known to inhibit actin polymerization, and its phosphorylation results in a decline of this inhibitory function (48). In this setting, actin monomers are released from the phosphorylated Hsp25 to self-associate to form fibrillar actin. Since the increase in myocyte LPL activity at 4 hours corresponded to an enlargement in the F-actin/G-actin ratio, our data suggest that AMPK and p38 MAPK, through their control of Hsp25 and the actin cytoskeleton, act in

unison to facilitate LPL translocation to the myocyte cell surface.

To eliminate the possibility that the above changes are: a) an outcome of a direct cardio toxic effect of DZ, and b) a result of the myriad metabolic and hormonal changes that arise during diabetes, we used compounds to directly stimulate AMPK and p38 MAPK. AICAR is a cell permeable activator of AMPK (49). In neonatal myocytes, 0.5-1 mM AICAR is required to stimulate AMPK activity (50), whereas a concentration of up to 2 mM is essential for AMPK phosphorylation in adult myocytes (51). In the present study, 2 mM AICAR activated AMPK in a manner comparable to that seen with DZ. Prompt activation followed by a reduction to control levels. At present, the mechanism for this decrease in cardiomyocyte AMPK phosphorylation with time is unknown (given the absence of FA in the myocyte incubation medium). An increase in energy charge due to amplification in glucose uptake, and the limited demand for energy in these non-beating quiescent myocytes are potential explanations. Similar to DZ, there was a close relationship between AMPK activation, p38 MAPK and Hsp25 phosphorylation, and the increase in cardiomyocyte heparin releasable LPL activity after exposure to AICAR. A different approach used thrombin to activate p38 MAPK. It should be noted that the more traditional methods to activate p38 MAPK includes sorbitol and anisomycin; however, sorbitol is also known to activate AMPK (52), whereas anisomycin is shown to cause insulin resistance (53). Thrombin, without affecting AMPK phosphorylation, had a robust effect to provoke cardiomyocyte p38 MAPK, likely through PAR-4 receptor and c-Src tyrosine kinase activation (54). More importantly, p38 MAPK phosphorylation was followed by nuclear translocation, phosphorylation of Hsp25, actin cytoskeleton reorganization and an increase in cell surface LPL activity. As the p38 MAPK inhibitor SB202190 and siRNA mediated

inhibition of p38 MAPK blocked the effects of thrombin and AICAR respectively on Hsp25 and LPL activity, our data suggest that F-actin polymerization produced by activation of p38 MAPK is an important means by which vesicle transport of LPL is made possible.

In summary, we propose that in addition to its direct role in promoting FA oxidation, AMPK recruitment of LPL to the cardiomyocyte cell surface could represent an immediate compensatory response by the heart to guarantee FA supply when glucose utilization is compromised. The mechanism underlying this process embraces p38 MAPK activation, and an increase in actin cytoskeleton polymerization (Fig. 10). Interestingly, the actin cytoskeleton also plays a key role in promoting insulin-induced GLUT 4 translocation. At present, the process of LPL vesicular movement along the actin filament network is unknown, and merits further investigation. Understanding this mechanism could lead to strategies that overcome contractile dysfunction following diabetes. This is because changes in cardiac LPL activity may predispose people with diabetes to premature death from cardiac disease. In mice, both cardiac specific overexpression [with its attendant lipid deposition, muscle fiber degeneration, and proliferation of mitochondria and peroxisomes, (55)], and knockout [associated with cardiac interstitial and perivascular fibrosis (56)] of LPL have been implicated in cardiac dysfunction.

Limitations of the study. One limitation of this study is the lack of mouse models supporting the role of AMPK/p38 MAPK in regulating LPL recruitment to the cardiomyocyte cell surface. Transgenic mice overexpressing MAPK kinase 6 and MKP-1 are available, and could potentially be used in future studies. However, it should be noted that endothelium-bound heparin-releasable LPL activity was unchanged in both Type 1 and Type 2 diabetic mouse hearts (57). This

could be a consequence of genetic adaptation, or the excessive heart rate in control animals (~600 beats/min), permitting prior translocation of LPL from the cardiomyocyte to the coronary lumen to saturate all of the LPL HSPG binding sites.

ACKNOWLEDGMENTS

The studies described in this paper were supported by an operating grant from the Canadian Diabetes Association

REFERENCES

1. Stamler J, Vaccaro O, Neaton JD, Wentworth D (1993) Diabetes, other risk factors, and 12-yr cardiovascular mortality for men screened in the Multiple Risk Factor Intervention Trial. *Diabetes Care* 16:434-444
2. Wilson PW (2001) Diabetes mellitus and coronary heart disease. *Endocrinol Metab Clin North Am* 30:857-881
3. Bertoni AG, Tsai A, Kasper EK, Brancati FL (2003) Diabetes and idiopathic cardiomyopathy: a nationwide case-control study. *Diabetes Care* 26:2791-2795
4. Diamant M, Lamb HJ, Groeneveld Y, Endert EL, Smit JW, Bax JJ, Romijn JA, de Roos A, Radder JK (2003) Diastolic dysfunction is associated with altered myocardial metabolism in asymptomatic normotensive patients with well-controlled type 2 diabetes mellitus. *J Am Coll Cardiol* 42:328-335
5. Fein FS (1990) Diabetic cardiomyopathy. *Diabetes Care* 13:1169-1179
6. Fang ZY, Prins JB, Marwick TH (2004) Diabetic cardiomyopathy: evidence, mechanisms, and therapeutic implications. *Endocr Rev* 25:543-567
7. Rodrigues B, Cam MC, McNeill JH (1995) Myocardial substrate metabolism: implications for diabetic cardiomyopathy. *J Mol Cell Cardiol* 27:169-179
8. Golfman LS, Takeda N, Dhalla NS (1996) Cardiac membrane Ca(2+)-transport in alloxan-induced diabetes in rats. *Diabetes Res Clin Pract* 31 Suppl:S73-77
9. Lopaschuk GD (2002) Metabolic abnormalities in the diabetic heart. *Heart Fail Rev* 7:149-159
10. Yagyu H, Chen G, Yokoyama M, Hirata K, Augustus A, Kako Y, Seo T, Hu Y, Lutz EP, Merkel M, Bensadoun A, Homma S, Goldberg IJ (2003) Lipoprotein lipase (LpL) on the surface of cardiomyocytes increases lipid uptake and produces a cardiomyopathy. *J Clin Invest* 111:419-426
11. Chiu HC, Kovacs A, Blanton RM, Han X, Courtois M, Weinheimer CJ, Yamada KA, Brunet S, Xu H, Nerbonne JM, Welch MJ, Fettig NM, Sharp TL, Sambandam N, Olson KM, Ory DS, Schaffer JE (2005) Transgenic expression of fatty acid transport protein 1 in the heart causes lipotoxic cardiomyopathy. *Circ Res* 96:225-233
12. Finck BN, Lehman JJ, Leone TC, Welch MJ, Bennett MJ, Kovacs A, Han X, Gross RW, Kozak R, Lopaschuk GD, Kelly DP (2002) The cardiac phenotype induced by PPARalpha overexpression mimics that caused by diabetes mellitus. *J Clin Invest* 109:121-130
13. Chiu HC, Kovacs A, Ford DA, Hsu FF, Garcia R, Herrero P, Saffitz JE, Schaffer JE (2001) A novel mouse model of lipotoxic cardiomyopathy. *J Clin Invest* 107:813-822
14. Belke DD, Larsen TS, Gibbs EM, Severson DL (2000) Altered metabolism causes cardiac dysfunction in perfused hearts from diabetic (db/db) mice. *Am J Physiol Endocrinol Metab* 279:E1104-1113
15. Eckel RH (1989) Lipoprotein lipase. A multifunctional enzyme relevant to common metabolic diseases. *N Engl J Med* 320:1060-1068
16. Pillarisetti S, Paka L, Sasaki A, Vanni-Reyes T, Yin B, Parthasarathy N, Wagner WD, Goldberg IJ (1997) Endothelial cell heparanase modulation of lipoprotein lipase activity. Evidence that heparan sulfate oligosaccharide is an extracellular chaperone. *J Biol Chem* 272:15753-15759
17. Augustus AS, Kako Y, Yagyu H, Goldberg IJ (2003) Routes of FA delivery to cardiac muscle: modulation of lipoprotein lipolysis alters uptake of TG-derived FA. *Am J Physiol Endocrinol Metab* 284:E331-339

18. Teusink B, Voshol PJ, Dahlmans VE, Rensen PC, Pijl H, Romijn JA, Havekes LM (2003) Contribution of fatty acids released from lipolysis of plasma triglycerides to total plasma fatty acid flux and tissue-specific fatty acid uptake. *Diabetes* 52:614-620
19. Mulder M, Lombardi P, Jansen H, van Berkel TJ, Frants RR, Havekes LM (1993) Low density lipoprotein receptor internalizes low density and very low density lipoproteins that are bound to heparan sulfate proteoglycans via lipoprotein lipase. *J Biol Chem* 268:9369-9375
20. Hardie DG (2003) Minireview: the AMP-activated protein kinase cascade: the key sensor of cellular energy status. *Endocrinology* 144:5179-5183
21. An D, Pulinilkunnil T, Qi D, Ghosh S, Abrahani A, Rodrigues B (2005) The metabolic "switch" AMPK regulates cardiac heparin-releasable lipoprotein lipase. *Am J Physiol Endocrinol Metab* 288:E246-253
22. Foy JM, Furman BL (1973) Effect of single dose administration of diuretics on the blood sugar of alloxan-diabetic mice or mice made hyperglycaemic by the acute administration of diazoxide. *Br J Pharmacol* 47:124-132
23. Pulinilkunnil T, Qi D, Ghosh S, Cheung C, Yip P, Varghese J, Abrahani A, Brownsey R, Rodrigues B (2003) Circulating triglyceride lipolysis facilitates lipoprotein lipase translocation from cardiomyocyte to myocardial endothelial lining. *Cardiovasc Res* 59:788-797
24. Rodrigues B, Cam MC, Jian K, Lim F, Sambandam N, Shepherd G (1997) Differential effects of streptozotocin-induced diabetes on cardiac lipoprotein lipase activity. *Diabetes* 46:1346-1353
25. Sambandam N, Abrahani MA, St Pierre E, Al-Atar O, Cam MC, Rodrigues B (1999) Localization of lipoprotein lipase in the diabetic heart: regulation by acute changes in insulin. *Arterioscler Thromb Vasc Biol* 19:1526-1534
26. Qi D, Kuo KH, Abrahani A, An D, Qi Y, Heung J, Kewalramani G, Pulinilkunnil T, Ghosh S, Innis SM, Rodrigues B (2006) Acute intralipid infusion reduces cardiac luminal lipoprotein lipase but recruits additional enzyme from cardiomyocytes. *Cardiovasc Res* 72:124-133
27. Qi D, Pulinilkunnil T, An D, Ghosh S, Abrahani A, Pospisilik JA, Brownsey R, Wambolt R, Allard M, Rodrigues B (2004) Single-dose dexamethasone induces whole-body insulin resistance and alters both cardiac fatty acid and carbohydrate metabolism. *Diabetes* 53:1790-1797
28. Pulinilkunnil T, Abrahani A, Varghese J, Chan N, Tang I, Ghosh S, Kulpa J, Allard M, Brownsey R, Rodrigues B (2003) Evidence for rapid "metabolic switching" through lipoprotein lipase occupation of endothelial-binding sites. *J Mol Cell Cardiol* 35:1093-1103
29. Haugland RP, You W, Paragas VB, Wells KS, DuBose DA (1994) Simultaneous visualization of G- and F-actin in endothelial cells. *J Histochem Cytochem* 42:345-350
30. Pulinilkunnil T, An D, Ghosh S, Qi D, Kewalramani G, Yuen G, Virk N, Abrahani A, Rodrigues B (2005) Lysophosphatidic acid-mediated augmentation of cardiomyocyte lipoprotein lipase involves actin cytoskeleton reorganization. *Am J Physiol Heart Circ Physiol* 288:H2802-2810
31. Kewalramani G, An D, Kim MS, Ghosh S, Qi D, Abrahani A, Pulinilkunnil T, Sharma V, Wambolt RB, Allard MF, Innis SM, Rodrigues B (2007) AMPK control of myocardial fatty acid metabolism fluctuates with the intensity of insulin-deficient diabetes. *J Mol Cell Cardiol* 42:333-342
32. Li J, Miller EJ, Ninomiya-Tsuji J, Russell RR, 3rd, Young LH (2005) AMP-activated protein kinase activates p38 mitogen-activated protein kinase by increasing recruitment of p38 MAPK to TAB1 in the ischemic heart. *Circ Res* 97:872-879

33. Ewart HS, Severson DL (1999) Insulin and dexamethasone stimulation of cardiac lipoprotein lipase activity involves the actin-based cytoskeleton. *Biochem J* 340 (Pt 2):485-490
34. Zheng C, Lin Z, Zhao ZJ, Yang Y, Niu H, Shen X (2006) MAPK-activated protein kinase-2 (MK2)-mediated formation and phosphorylation-regulated dissociation of the signal complex consisting of p38, MK2, Akt, and Hsp27. *J Biol Chem* 281:37215-37226
35. Camps L, Reina M, Llobera M, Vilaro S, Olivecrona T (1990) Lipoprotein lipase: cellular origin and functional distribution. *Am J Physiol* 258:C673-681
36. Otarod JK, Goldberg IJ (2004) Lipoprotein lipase and its role in regulation of plasma lipoproteins and cardiac risk. *Curr Atheroscler Rep* 6:335-342
37. Hardie DG, Hawley SA (2001) AMP-activated protein kinase: the energy charge hypothesis revisited. *Bioessays* 23:1112-1119
38. Hardie DG, Carling D (1997) The AMP-activated protein kinase--fuel gauge of the mammalian cell? *Eur J Biochem* 246:259-273
39. Hong SP, Leiper FC, Woods A, Carling D, Carlson M (2003) Activation of yeast Snf1 and mammalian AMP-activated protein kinase by upstream kinases. *Proc Natl Acad Sci U S A* 100:8839-8843
40. Hayashi T, Hirshman MF, Fujii N, Habinowski SA, Witters LA, Goodyear LJ (2000) Metabolic stress and altered glucose transport: activation of AMP-activated protein kinase as a unifying coupling mechanism. *Diabetes* 49:527-531
41. Russell RR, 3rd, Bergeron R, Shulman GI, Young LH (1999) Translocation of myocardial GLUT-4 and increased glucose uptake through activation of AMPK by AICAR. *Am J Physiol* 277:H643-649
42. Marsin AS, Bertrand L, Rider MH, Deprez J, Beauloye C, Vincent MF, Van den Berghe G, Carling D, Hue L (2000) Phosphorylation and activation of heart PFK-2 by AMPK has a role in the stimulation of glycolysis during ischaemia. *Curr Biol* 10:1247-1255
43. Luiken JJ, Coort SL, Willems J, Coumans WA, Bonen A, van der Vusse GJ, Glatz JF (2003) Contraction-induced fatty acid translocase/CD36 translocation in rat cardiac myocytes is mediated through AMP-activated protein kinase signaling. *Diabetes* 52:1627-1634
44. Kudo N, Barr AJ, Barr RL, Desai S, Lopaschuk GD (1995) High rates of fatty acid oxidation during reperfusion of ischemic hearts are associated with a decrease in malonyl-CoA levels due to an increase in 5'-AMP-activated protein kinase inhibition of acetyl-CoA carboxylase. *J Biol Chem* 270:17513-17520
45. Watt MJ, Steinberg GR, Chen ZP, Kemp BE, Febbraio MA (2006) Fatty acids stimulate AMP-activated protein kinase and enhance fatty acid oxidation in L6 myotubes. *J Physiol* 574:139-147
46. Wu Y, Song P, Xu J, Zhang M, Zou MH (2007) Activation of protein phosphatase 2A by palmitate inhibits AMP-activated protein kinase. *J Biol Chem* 282:9777-9788
47. Tan Y, Rouse J, Zhang A, Cariati S, Cohen P, Comb MJ (1996) FGF and stress regulate CREB and ATF-1 via a pathway involving p38 MAP kinase and MAPKAP kinase-2. *Embo J* 15:4629-4642
48. Dai T, Natarajan R, Nast CC, LaPage J, Chuang P, Sim J, Tong L, Chamberlin M, Wang S, Adler SG (2006) Glucose and diabetes: effects on podocyte and glomerular p38MAPK, heat shock protein 25, and actin cytoskeleton. *Kidney Int* 69:806-814
49. Corton JM, Gillespie JG, Hawley SA, Hardie DG (1995) 5-aminoimidazole-4-carboxamide ribonucleoside. A specific method for activating AMP-activated protein kinase in intact cells? *Eur J Biochem* 229:558-565

50. Chan AY, Soltys CL, Young ME, Proud CG, Dyck JR (2004) Activation of AMP-activated protein kinase inhibits protein synthesis associated with hypertrophy in the cardiac myocyte. *J Biol Chem* 279:32771-32779
51. Chabowski A, Momken I, Coort SL, Calles-Escandon J, Tandon NN, Glatz JF, Luiken JJ, Bonen A (2006) Prolonged AMPK activation increases the expression of fatty acid transporters in cardiac myocytes and perfused hearts. *Mol Cell Biochem* 288:201-212
52. Smith JL, Patil PB, Fisher JS (2005) AICAR and hyperosmotic stress increase insulin-stimulated glucose transport. *J Appl Physiol* 99:877-883
53. Hilder TL, Baer LA, Fuller PM, Fuller CA, Grindeland RE, Wade CE, Graves LM (2005) Insulin-independent pathways mediating glucose uptake in hindlimb-suspended skeletal muscle. *J Appl Physiol* 99:2181-2188
54. Kanda Y, Watanabe Y (2005) Thrombin-induced glucose transport via Src-p38 MAPK pathway in vascular smooth muscle cells. *Br J Pharmacol* 146:60-67
55. Levak-Frank S, Radner H, Walsh A, Stollberger R, Knipping G, Hoefler G, Sattler W, Weinstock PH, Breslow JL, Zechner R (1995) Muscle-specific overexpression of lipoprotein lipase causes a severe myopathy characterized by proliferation of mitochondria and peroxisomes in transgenic mice. *J Clin Invest* 96:976-986
56. Augustus AS, Buchanan J, Park TS, Hirata K, Noh HL, Sun J, Homma S, D'Armiento J, Abel ED, Goldberg IJ (2006) Loss of lipoprotein lipase-derived fatty acids leads to increased cardiac glucose metabolism and heart dysfunction. *J Biol Chem* 281:8716-8723
57. Neitzel AS, Carley AN, Severson DL (2003) Chylomicron and palmitate metabolism by perfused hearts from diabetic mice. *Am J Physiol Endocrinol Metab* 284:E357-365

Table 1. Effect of AICAR on cardiomyocyte LPL activity

LPL activity (nmol/hr/10 ⁶ cells)	(min)	AICAR				
		0	30	60	90	120
-Heparin		1678 ± 94	1724 ± 32	1825 ± 164	1832 ± 73	1798 ± 92
+Heparin		2215 ± 85	2305 ± 48	3725 ± 256	5624 ± 75*	5782 ± 115*

Myocytes were prepared as described in the methods. AICAR (2 mM) was added to the culture medium, and myocytes kept for 30-120 minutes. Following the indicated times, myocyte basal LPL activity released into the medium was measured. To release surface-bound LPL activity, heparin (8 U/ml; 1min) was added to the culture plates, aliquots of cell medium removed, separated by centrifugation, and assayed for LPL activity. Results are the mean \pm SEM of 3 rats in each group. *Significantly different from control, $P < 0.05$.

FIGURE LEGENDS

FIG. 1. Blood glucose and LPL activity subsequent to Diazoxide (DZ). Animals were treated with DZ (100 mg/kg, i.p.), and blood samples collected over a period of 4 h. Blood glucose was determined using a glucometer and glucose test strips (A). Results are the means \pm SE of 3 rats in each group. At the indicated times, hearts from control and DZ treated animals were also isolated and perfused in the non-recirculating retrograde mode. Thereafter, coronary luminal LPL was released with heparin (5 U/ml). Coronary effluents were collected (for 10 s) over 5 mins, but only peak LPL activities are illustrated. LPL activity was assayed using radiolabeled triolein. The lower panel (B) illustrates peak heparin-releasable LPL activity released after varying durations of DZ (0-240 min). Results are the means \pm SE of 3 rats in the 0 and 240 min group. In the other groups, only a representative value is indicated. *Significantly different from untreated control (0 min), $P < 0.05$.

FIG. 2. Alterations in AMPK phosphorylation in hearts isolated from Diazoxide treated animals or control myocytes treated with fatty acids. Following DZ for different intervals, total or phosphorylated AMPK- α was determined immediately upon removal of the heart using Western blotting (A). Total and phospho-AMPK- α were measured using rabbit AMPK- α or phospho-AMPK (Thr-172) antibodies respectively. Blood samples were also collected over a period of 4-h after administration of DZ. After centrifugation, plasma was separated for determination of NEFA (B). Panel C represents total and phospho-AMPK- α following incubation of plated myocytes (0.4×10^6 cells) with 0.5-1.5 mM albumin bound palmitic acid (1:2). Data are means \pm SE of 3 rats in each group. *Significantly different from control (0 min), $P < 0.05$.

FIG. 3. Time dependent changes in phosphorylation of p38 MAPK and Hsp25 and actin polymerization following DZ. Cytosolic and nuclear p38 MAPK were evaluated using rabbit p38 MAPK or phospho-p38 MAPK (Thr180/Tyr182) antibodies (A). Total or phosphorylated Hsp25 were also determined immediately upon removal of the heart using rabbit Hsp25 or phospho-Hsp25 (S86) antibodies, and Western blotting (B). Data are means \pm SE of 3 different hearts in each group. *Significantly different from control, $P < 0.05$. Cardiac actin rearrangement following DZ was determined using a G-actin/F-actin in vivo assay kit (C). Total actin was centrifuged to isolate F-actin (pellet) and G-actin (supernatant). The ratio of F-actin/G-actin was determined using western blotting and densitometry. An increase in F-to-G actin ratio was assumed to represent polymerization of actin filaments. Data are means \pm SE of 3 different hearts in each group. *Significantly different from control (0 min), #Significantly different from DZ (60 min), $P < 0.05$.

FIG. 4. Consequence of AMPK activation using AICAR. Cardiomyocytes were plated on laminin-coated culture plates. Cells were maintained using Media-199, and incubated at 37°C under an atmosphere of 95% O₂/5% CO₂ for 16 hours. Subsequently, 5-aminoimidazole-4-carboxamide-1- β -D-ribofuranoside (2 mM) was added to the culture medium. At the indicated times, protein was extracted to determine AMPK (A), p38 (B), and Hsp25 (C) (both total and phosphorylated) using Western Blotting. Data are means \pm SE; n=3 myocyte preparations from different animals. *Significantly different from control (0 min), $P < 0.05$.

FIG. 5. Effect of inhibiting p38 MAPK on AICAR induced phosphorylation of Hsp25 and increase in heparin-releasable LPL activity. Cardiomyocytes were pre-incubated in the absence or presence of a p38 MAPK inhibitor (SB202190, 20 μ M) added to the culture medium for 60 min. Subsequently, the myocytes were exposed to AICAR (2 mM). At the indicated times (90 and 120 min), protein was extracted to determine Hsp25 (both total and phosphorylated) using Western Blotting (A). Myocyte LPL activity was also measured after incubations with both SB202190 (pre-incubation for 60 min) and AICAR (90 and 120 min). To release surface-bound LPL activity, heparin (8 U/mL; 1 min) was added to the culture plates, aliquots of cell medium removed, separated by centrifugation, and assayed for LPL activity (B). Data are means \pm SE; n=3 myocyte preparations from different animals. *Significantly different from control (0 min), #Significantly different from AICAR alone, $P < 0.05$.

FIG. 6. p38 MAPK and Hsp25 phosphorylation following incubation of cardiomyocytes with thrombin. Cardiomyocytes were incubated with thrombin (0.05 U/ml) added to the culture medium, and myocytes kept for 0-60 minutes. At the indicated times, cytosolic (A) and nuclear (B) protein was extracted to determine p38 MAPK. Total and phosphorylated Hsp25 were also determined at the indicated times using Western Blotting (C). Cytosolic phospho-AMPK- α was also determined after incubation with thrombin (A, inset). Data are means \pm SE; n=3 myocyte preparations from different animals. *Significantly different from control, $P < 0.05$.

FIG. 7. Effect of thrombin on Hsp25 phosphorylation and heparin-releasable LPL activity in cardiomyocytes. Myocytes were prepared as described in the methods. Thrombin (0.05 U/ml) was added to the culture medium, and myocytes kept for 30 and 60 minutes. Following the indicated times, protein was extracted to determine Hsp25 (both total and phosphorylated) using Western Blotting (A). Myocyte basal LPL activity released into the medium was also measured following incubation with thrombin (30 and 60 min). To release surface-bound LPL activity, heparin (8 U/mL; 1 min) was added to the culture plates, aliquots of cell medium removed, separated by centrifugation, and assayed for LPL activity (B). Myocytes were also pre-incubated with a p38 MAPK inhibitor (SB202190, 20 μ M) for 60 min prior to addition of thrombin (30 and 60 min) and subsequent determination of Hsp25 (A) and LPL activity (B). Data are means \pm SE; n=3 myocyte preparations from different animals. *Significantly different from control (0 min), #Significantly different from thrombin alone, $P < 0.05$.

FIG. 8. Myocyte actin rearrangement following thrombin. Thrombin (0.05 U/ml) was added to plated myocytes, and the cells kept for 30 and 60 minutes. Myocytes were fixed, permeabilized and double stained with DNAaseI AlexaFluor®594 and Rhodamine®488 Phalloidin to colocalize monomeric globular actin (red, G-actin), and polymerized filamentous actin (green, F-actin). The merged image of F-actin and G-actin is described in the third panel. Myocytes were also pre-incubated with a p38 MAPK inhibitor (SB202190, 20 μ M) for 60 min prior to addition of thrombin (30 and 60 min) and subsequent determination of F-actin and G actin. Data is from a representative experiment done twice.

FIG. 9. Silencing of p38 MAPK by siRNA. siRNA transfection of p38 MAPK in cardiomyocytes was carried out using a kit from Santa Cruz. Plated myocytes were exposed to the siRNA (or scrambled, Scr). The inset depicts transfection efficiency. After this, AICAR (2 mM) was added to the culture medium for 2h and p38 MAPK (A), Hsp25 (B), and LPL activity

(C) were evaluated. Data are means \pm SE; n=3 myocyte preparations from different animals. *Significantly different from control, #Significantly different from AICAR treated control, $P<0.05$.

FIG. 10. AMPK recruitment of LPL to the cardiomyocyte cell surface. Following diabetes and activation of AMPK, p38 MAPK is phosphorylated and transferred to the nucleus to activate MAPKAP kinase 2, which is then exported to phosphorylate Hsp25. Actin monomers are released from the phosphorylated Hsp25 to self-associate to form fibrillar actin. Vesicles containing LPL then move along the actin filament network, and eventually bind to heparan sulfate proteoglycans on the plasma membrane. From here, LPL is transported onto HSPG binding sites on the luminal surface of the capillary endothelium.

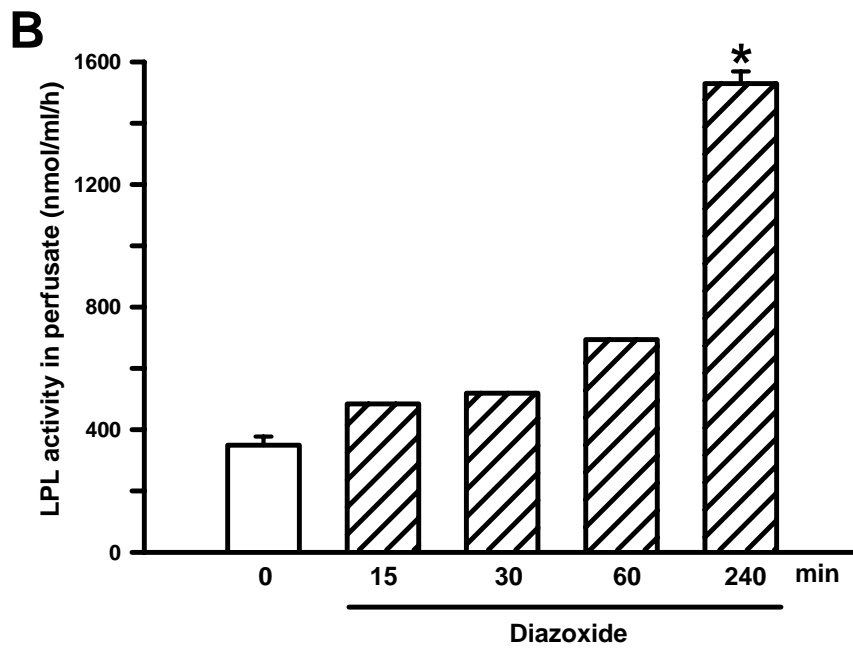
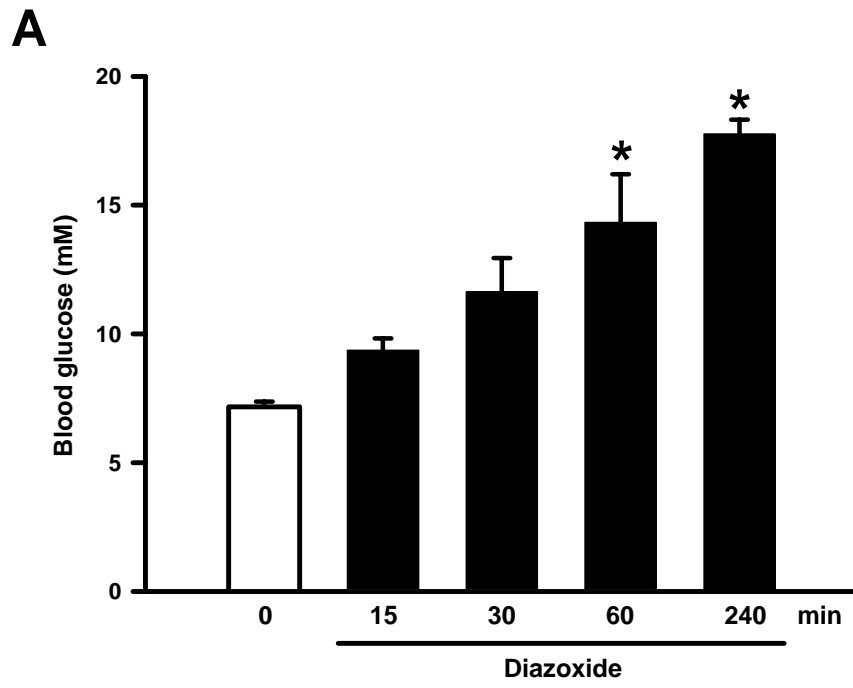


Fig.1

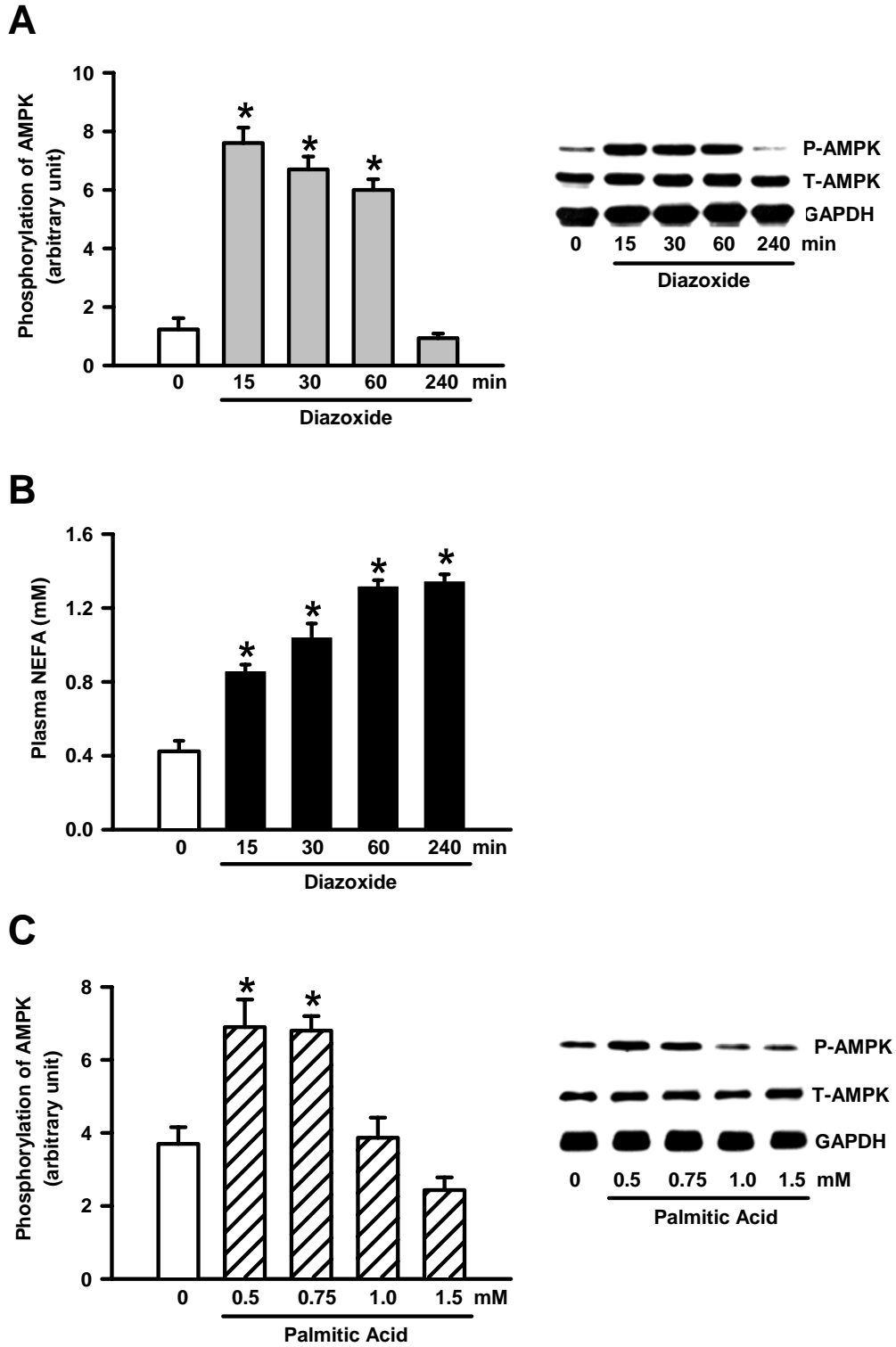


Fig. 2

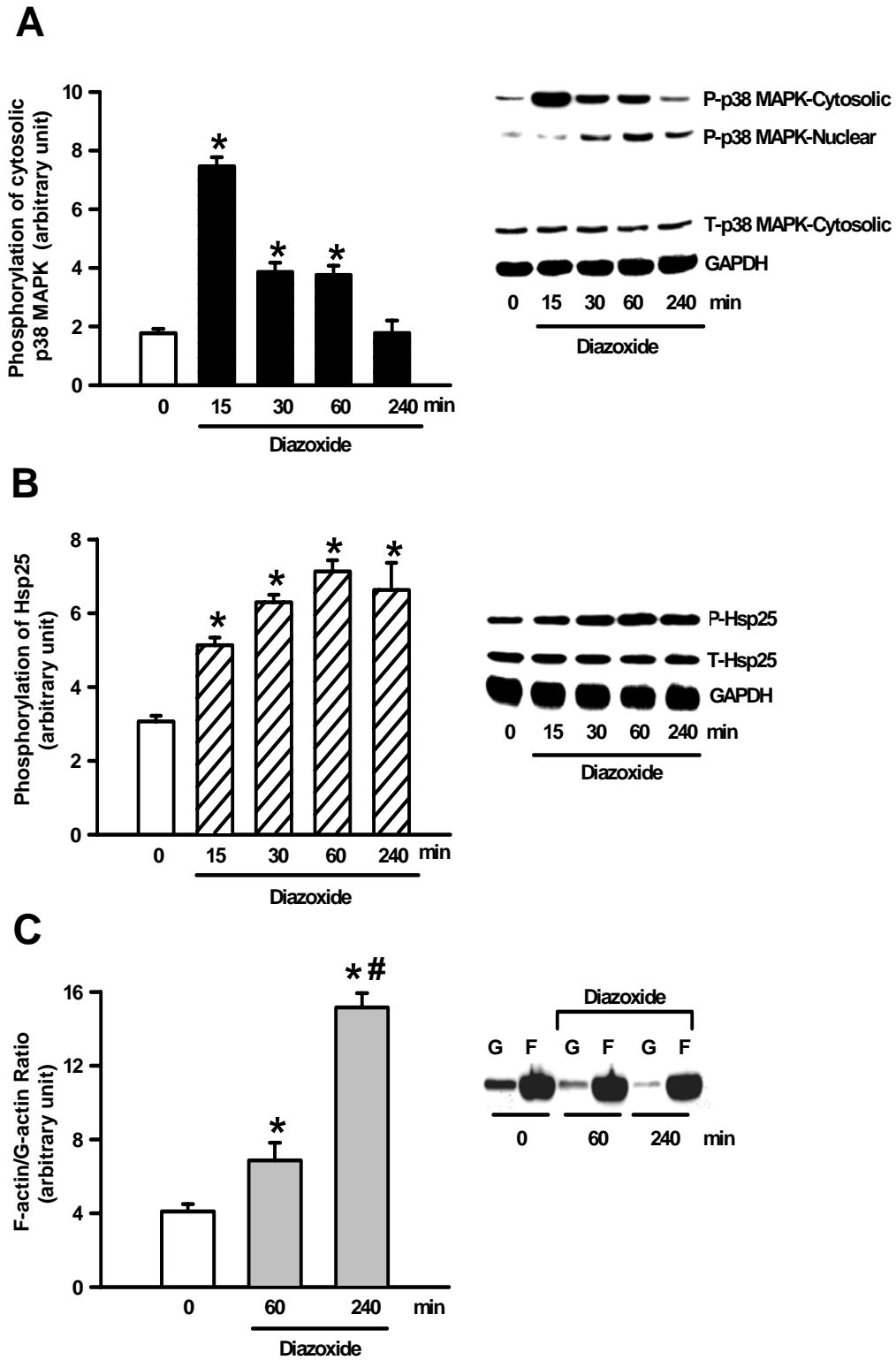


Fig.3

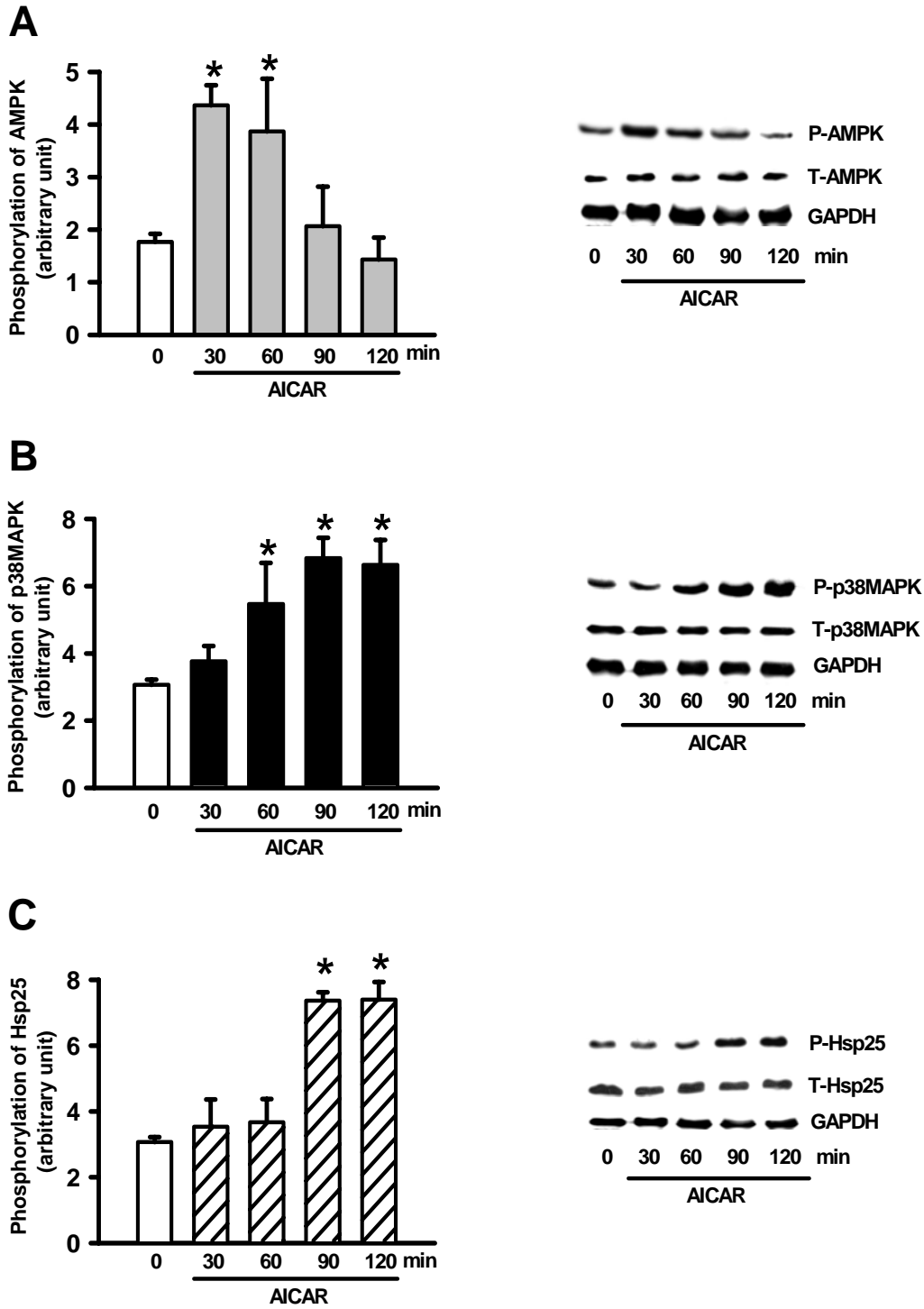
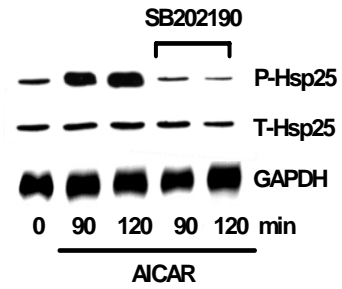
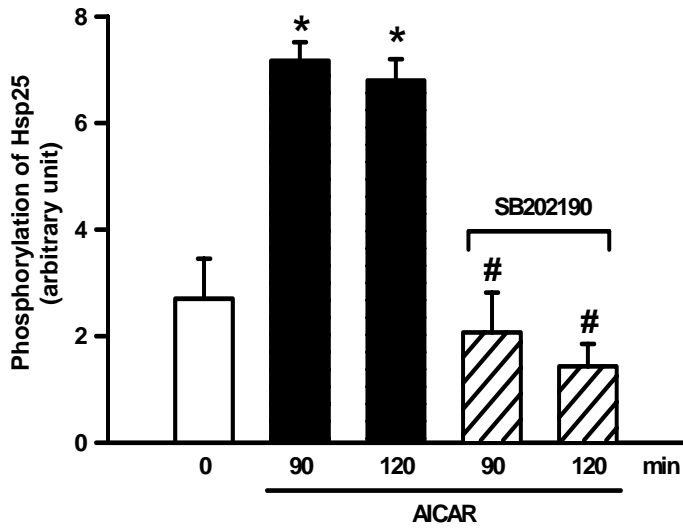


Fig. 4

A



B

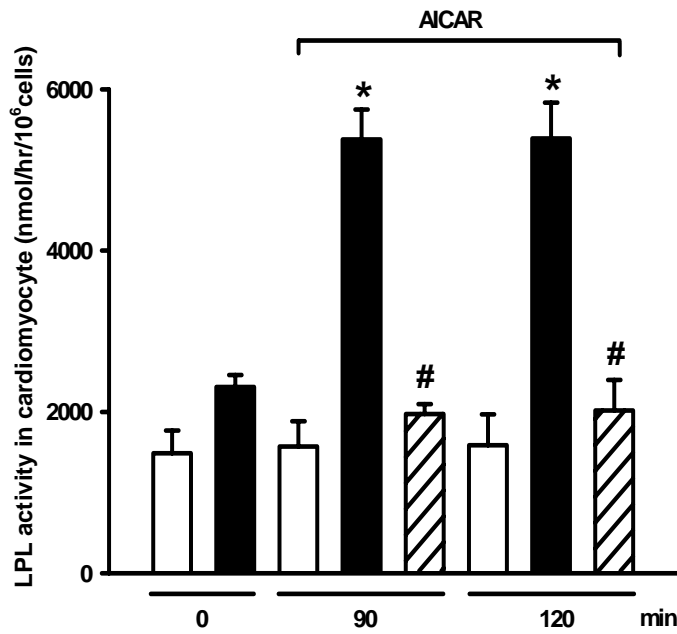
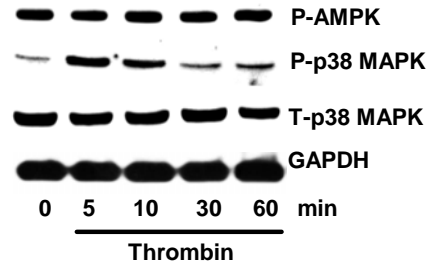
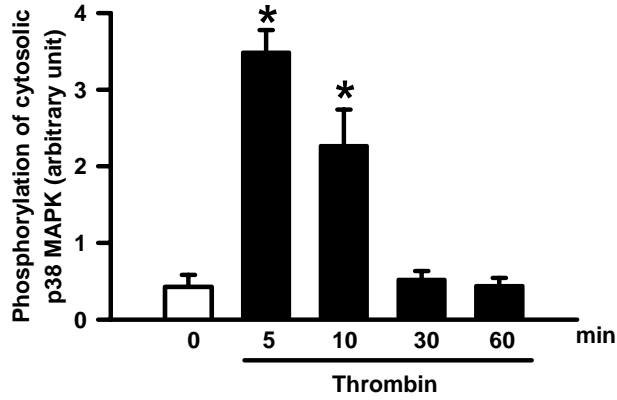
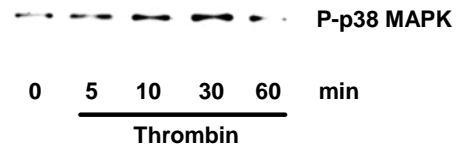
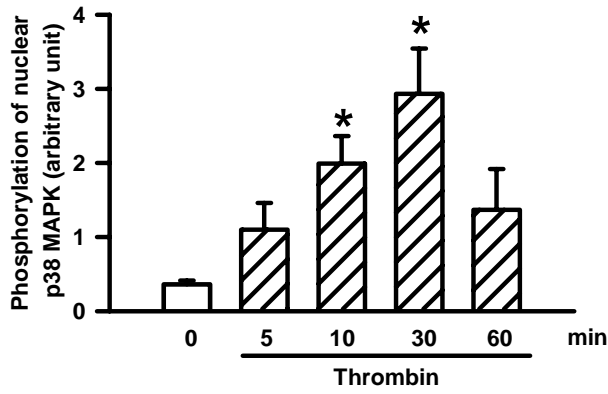


Fig.5

A



B



C

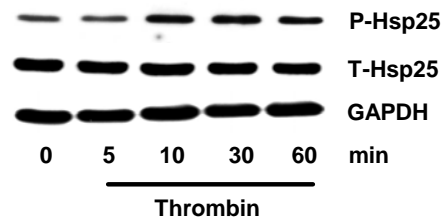
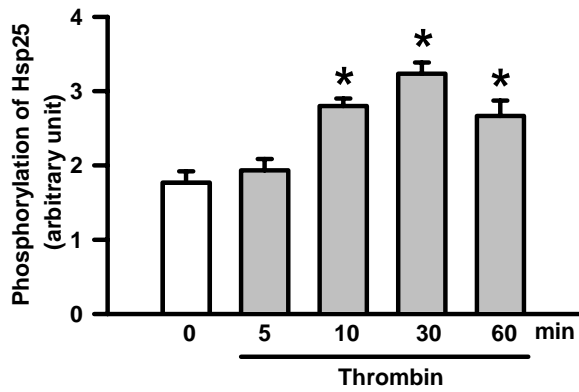


Fig. 6

